Upper bound for a three-photon excitation cross section in atomic argon in the ultraviolet regime

Noshir M. Khambatta and Leon J. Radziemski
Department of Physics, New Mexico State University, Las Cruces, New Mexico 88003

S. N. Dixit
Lawrence Livermore National Laboratory, Livermore, California 94550

(Received 27 September 1988; revised manuscript received 21 December 1988)

A scheme of evaluating a generalized three-photon excitation cross section $\sigma_{(3)}$ in neutral atomic argon at 3144.67 Å is outlined. Three photons at this wavelength can excite the neutral argon atoms from the ground $3p^6\,{}^1S_0$ state to the $3p^5 4s'[1/2]_1^0$ state. The fourth photon will ionize the argon atoms. Assuming linear polarization of the incident laser radiation, contributions from several channels in various energy-level schemes are summed in the evaluation of the transition probability. For a laser linewidth of $\Delta\lambda_L = 1$ Å, our maximum numerical value of the computed result for the three-photon excitation cross section is $\sigma_{(3)} = 1.414\times10^{-80}$ cm^6 s^2.

I. INTRODUCTION

One potential scheme for generating an ionized path in the atmosphere is via ionization of argon, a 1% volume constituent, well mixed up to 10 km. The realization of that scheme commences with the calculations of the multiple-photon excitation and ionization rates for argon. Single-photon photoionization of argon would occur at wavelengths that would not penetrate the atmosphere.[1] We have chosen to investigate a scheme which utilizes the intermediate resonance with the $3p^5 4s'[\frac{1}{2}]_1^0$ state. This would correspond to a three-photon excitation wavelength of 3144.67 Å (vacuum wavelength), a laser which does not now exist. However, the free-electron laser is potentially tunable in this region, so the calculations are relevant.

Using the standard perturbation theory techniques of nonresonant multiple-photon excitation in atoms,[2,3] we consider aspects of three-photon excitation in atomic argon at a wavelength of 3144.67 Å. From a knowledge of the energy-level tables of atomic argon and its atomic parameters (i.e., transition probabilities and transition wavelengths),[4–7] we outline a method of arriving at the three-photon transition rate (probability per unit time) and hence the generalized three-photon excitation cross section in argon at a wavelength of 3144.67 Å.

II. THEORY

A partial energy-level diagram of neutral atomic argon (Ar I) is shown in Fig. 1. Three photons at a wavelength of 3144.67 Å will excite the neutral argon atoms from the ground $3p^6\,{}^1S_0$ state to the $3p^5 4s'[\frac{1}{2}]_1^0$ state. The fourth photon at the same wavelength will ionize the argon atoms. Several schemes of excitation have been considered and their contributions summed in the evaluation of the transition rate. From Lambropoulos[2] the expression for the transition probability $W^{(3)}$ (in s^{-1}) for a three-photon bound-bound excitation is

$$W_{f,g}^{(3)} = (2\pi)(2\pi\alpha)^3 F^2 F(\omega_L)\omega_L^3 \left|\sum_{1,2} M_{1,2}^{(3)}\right|^2 , \quad (1)$$

where

$$\sum_{1,2} M_{1,2}^{(3)} = \sum_{1,2} \frac{\langle f|r^\lambda|2\rangle\langle 2|r^\lambda|1\rangle\langle 1|r^\lambda|g\rangle}{(\omega_2-\omega_g-2\omega_L)(\omega_1-\omega_g-\omega_L)} , \quad (2)$$

where g and f denote the ground and the final state of the atom, respectively, α is the fine-structure constant ($\frac{1}{137.036}$), F is the total photon flux measured in number of photons per cm^2 per second, $F(\omega_L)$ is the number of pho-

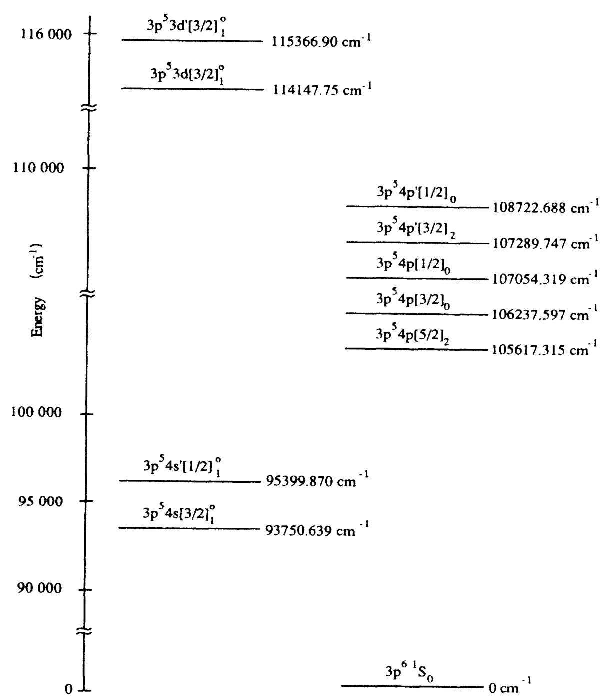

FIG. 1. Partial energy-level diagram of atomic argon (Ar I).

tons per cm^2 per second per unit bandwidth of the incident exciting laser, ω_L is the angular frequency of the exciting incident laser, $\langle |r^\lambda| \rangle$ are the dipole transition matrix elements, connecting the virtual states, and $\omega_2-\omega_g-2\omega_L$ and $\omega_1-\omega_g-\omega_L$ are the angular frequency detuning factors. $F(\omega_L)$ may be further expressed in terms of a lineshape function $g(\omega_L)$ as

$$F(\omega_L)=g(\omega_L)F \ , \tag{3}$$

where $g(\omega_L)$ is the line-shape function at the center of the line, given by the expression

$$g(\omega_L)=\frac{2\sqrt{\ln(2)/\pi}}{[2(\Delta\omega_L)^2+(\Delta\omega_T)^2]^{1/2}} \ , \tag{4}$$

where $\Delta\omega_L$ is the incident exciting laser bandwidth [full width at half maximum (FWHM)] (in s^{-1}) and $\Delta\omega_T$ is the transition Doppler bandwidth (FWHM) (in s^{-1}). If I is the incident laser irradiance in W/cm^2, then F may be expressed as

$$F=I/h\nu \ (\text{photons}\, \text{cm}^{-2}\, \text{s}^{-1}) \ , \tag{5}$$

where $h\nu$ is the energy of the incident laser photon.

III. THE EXCITATION SCHEMES

Due to the intrinsic nature of the energy-level diagram of neutral argon, we selected the six schemes as detailed below, for their contributions to the dipole transition matrix elements in the transition probability calculations. Various other schemes involving higher levels like the $3p^55p$, $3p^56p$, and $3p^57p$ were investigated and their contributions to the dipole transition matrix elements were found to be 2 to 3 orders of magnitude less than the numerical contributions of the chosen six schemes, and so were neglected. In short, we adopted the truncated summation approach to the infinite sums over virtual intermediate states $|1\rangle$ and $|2\rangle$, in Eq. (2). The choice of the virtual intermediate states in all the six schemes were made by the fact that computations were strictly performed for linear polarization of the incident exciting radiation. We outline below schemes I–VI.

In scheme I the ground state is the $3p^6\,{}^1S_0$ state symbolically denoted as $|g\rangle$. The first intermediate state is chosen to be the $3p^54s[\frac{3}{2}]_1^0$ state, symbolically denoted as $|1\rangle$. The second intermediate state denoted as $|2\rangle$, is the collective configuration of five levels belonging to the $3p^54p$ state as shown in Fig. 2. Angular momentum selection rules for linearly polarized incident radiation, dictated the choice of these five levels. The final state is the $3p^54s'[\frac{1}{2}]_1^0$ state, symbolically denoted as $|f\rangle$. In schemes II, III, IV, V, and VI, the ground state $|g\rangle$, the intermediate state $|2\rangle$, and the final state $|f\rangle$, are the same as those of scheme I. Only the intermediate state $|1\rangle$ is different for each of these schemes, and they are $3p^54s'[\frac{1}{2}]_1^0$, $3p^55s[\frac{3}{2}]_1^0$, $3p^55s'[\frac{3}{2}]_1^0$, $3p^53d[\frac{3}{2}]_1^0$, $3p^53d'[\frac{3}{2}]_1^0$, respectively.

Theoretically there are five channels in each scheme. A channel is defined as the transition from the ground state $|g\rangle$ to the intermediate state $|1\rangle$, then from state $|1\rangle$ to the intermediate state $|2\rangle$, and finally from state $|2\rangle$ to the final state $|f\rangle$. However, in schemes V and VI only two and three channels, respectively, have contributed to the dipole transition matrix elements as indicated in Table I, since the transition probabilities for other channels are not quoted in standard literature, to the best of our knowledge and research.

The numerical contribution of an individual channel to

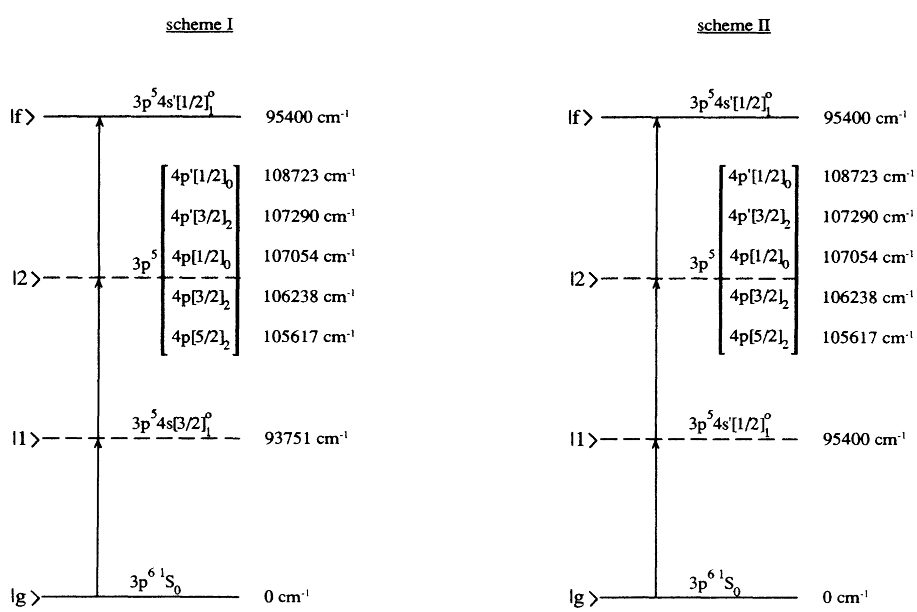

FIG. 2. Schematic representation of schemes I and II used in the evaluation of the radial matrix elements of the transition probability.

TABLE I. Tabulation of the magnitudes of the individual channel contributions to the evaluation of the transition probability for schemes I–VI. The entry 1.363[58] is an abbreviation for 1.363×10^{-58}. Units are in $cm^3\,s^2$.

Magnitudes	$3p^54p'[\frac{1}{2}]_0$	$3p^54p'[\frac{3}{2}]_2$	$3p^54p[\frac{1}{2}]_0$	$3p^54p[\frac{3}{2}]_2$	$3p^54p[\frac{5}{2}]_2$
$M_{\rm I}$	1.363[58]	4.913[58]	2.302[59]	3.553[58]	5.000[58]
$M_{\rm II}$	4.451[57]	3.001[57]	2.929[60]	9.759[58]	3.232[58]
$M_{\rm III}$	8.992[58]	6.546[59]	1.354[59]	2.706[58]	8.506[58]
$M_{\rm IV}$	4.418[58]	5.829[58]	1.092[60]	1.048[58]	2.020[59]
$M_{\rm V}$			3.705[59]		1.482[58]
$M_{\rm VI}$	1.989[57]		1.056[59]	1.558[58]	

the dipole transition matrix element is explained in detail below, and the contribution of each channel is summed to arrive at a scheme contribution to the dipole transition matrix elements. The contributions of these six schemes are then finally summed to arrive at a total numerical value of $\sum_{1,2} M_{1,2}^{(3)}$ in Eq. (2). We are aware of the fact that an individual channel contribution can be numerically positive or negative in magnitude, and that in reality an algebraic sum should be carried out over the intermediate states $|1\rangle$ and $|2\rangle$ in Eq. (2). However, in a computation scheme like ours there is no *a priori* way of determining the sign of a channel contribution, and so we have presumed it to be positive. This obviously results in a maximum possible value of $\sigma_{(3)}$ for a chosen set of exciting schemes, as we have indicated above.

IV. AN ILLUSTRATIVE EXAMPLE

We describe below a sample calculation to show how we arrive at a numerical contribution of a specific channel in a given scheme. All other channel contributions of all the selected schemes are tabulated in Table I. We assume that the incident laser radiation is strictly linearly polarized. In scheme I we select the channel

$$|g\rangle\rightarrow|1\rangle\rightarrow|2\rangle\{3p^54p'[\tfrac{1}{2}]_0\}\rightarrow|f\rangle\ .$$

For each transition in the channel, we evaluate the dipole transition matrix element (for linear polarization) via the expression[8,9]

$$|\langle\alpha LSJM_J|\hat{R}^{(\rm el)}|\alpha L'SJ'M_J'\rangle|^2 = (2J'+1)\begin{pmatrix} J & 1 & J' \\ -M_J & 0 & M_J'\end{pmatrix}^2 \frac{A^{(l)}}{\sigma^2(0.66702)}\frac{3}{\Delta E}\ , \quad (6)$$

where the squared transition matrix element on the left-hand side of Eq. (6) is expressed in units of a_0^2 (a_0 being the Bohr radius), $A^{(l)}$ is the transition probability in units of s^{-1}, σ is the transition wavelength in cm^{-1}, ΔE is the energy difference between the two levels in units of Ry, and the term in large parentheses is the Wigner $3j$ symbol of interest.

For $\langle 1|r^\lambda|g\rangle$,

$$J=0,\ M_J=0 \text{ and } J'=1,\ M_J'=0\ ,$$

$$A^{(l)}=1.19\times10^8\ s^{-1},\quad \sigma^2=8.789\times10^9\ cm^{-2}\ ,$$

$$\Delta E=0.854\ \text{Ry}\ ,$$

$$\begin{pmatrix} 0 & 1 & 1\\ 0 & 0 & 0\end{pmatrix}^2=\frac{1}{3}\ .$$

This results in $|\langle 1|r^\lambda|g\rangle|^2\cong1.995\times10^{-18}\ cm^2$.

For $\langle 2\{3p^54p'[\frac{1}{2}]_0\}|r^\lambda|1\rangle$,

$$J=1,\ M_J=0 \text{ and } J'=0,\ M_J'=0\ ,$$

$$A^{(l)}=0.0024\times10^8\ s^{-1},\quad \sigma^2=2.243\times10^8\ cm^{-2}\ ,$$

$$\Delta E=0.136\ \text{Ry}\ .$$

This results in $|\langle 2\{3p^54p'[\frac{1}{2}]_0|r^\lambda|1\rangle|^2\cong3.315\times10^{-19}$ cm^2.

For $\langle f|r^\lambda|2\{3p^54p'[\frac{1}{2}]_0\}\rangle$

$$J=0,\ M_J=0 \text{ and } J'=1,\ M_J'=0\ ,$$

$$A^{(l)}=0.472\times10^8\ s^{-1},\quad \sigma^2=1.776\times10^8\ cm^{-2}\ ,$$

$$\Delta E=0.121\ \text{Ry}\ .$$

This results in

$$|\langle f|r^\lambda|2\{3p^54p'[\tfrac{1}{2}]_0\}\rangle|^2\cong2.764\times10^{-16}\ cm^2\ .$$

Also for our incident laser radiation

$$\lambda_L=3144.76\ \text{Å},\quad \omega_L=5.990\times10^{15}\ s^{-1}\ ,$$

$$\omega_1-\omega_g-\omega_L=1.167\times10^{16}\ s^{-1},\quad \omega_2-\omega_g-2\omega_L=8.499\times10^{15}\ s^{-1}\ ,$$

$$M_{\rm I}(3p^54p'[\tfrac{1}{2}]_0)=\frac{(2.764\times10^{-16})^{1/2}(3.315\times10^{-19})^{1/2}(2.764\times10^{-16})^{1/2}}{(8.499\times10^{15})(1.167\times10^{16})}\cong1.363\times10^{-58}\ cm^3\,s^2\ .$$

V. NUMERICAL RESULTS

Summing the contributions of all the schemes in Table I, we finally arrive at

$$\left|\sum_{1,2} M_{1,2}^{(3)}\right|\cong1.585\times10^{-56}\ cm^3\,s^2\ .$$

Rewriting Eq. (1), we have

$$W^{(3)}_{f,g}(\Delta\lambda_L,F)=(2\pi)\left[\frac{2\pi}{137.036}\right]^3(5.990\times10^{15})^3$$
$$\times|1.585\times10^{-56}|^2 g(\omega)F^3$$
$$\cong 3.270\times10^{-68} g(\omega)F^3 \quad (7)$$

in s^{-1} units. Typically if we assume a laser bandwidth of $\Delta\lambda_L=1$ Å, we can neglect the Doppler contribution in $g(\omega_L)$ in Eq. (4), to obtain $g(\omega_L)\cong 3.487\times10^{-13}$ s. With this

$$W^{(3)}_{f,g}(\Delta\lambda_L=1 \text{ Å}, F)\cong 1.414\times10^{-80}F^3 . \quad (8)$$

Again from Lambropoulos *et al.*,[2] for an N-photon process we have

$$W^{(N)}_{f,g}=\sigma_{(N)}F^N , \quad (9)$$

which for our case of $N=3$ reduces to

$$W^{(3)}_{f,g}=\sigma_{(3)}F^3 , \quad (10)$$

where $\sigma_{(3)}$ is the generalized three-photon excitation cross section. An elementary comparison shows us that

$$\sigma_{(3)}(1 \text{ Å})=1.414\times10^{-80} \text{ cm}^6\text{ s}^2 . \quad (11)$$

VI. A SIMPLE APPLICATION

The above numerical value of $\sigma_{(3)}$ can be utilized to give an order of magnitude estimate of the number of excited argon atoms in the $3p^5 4s'[\frac{1}{2}]^0_1$ level due to the three-photon excitation. Neglecting losses due to radiation and collisions and ionization for the duration of our laser pulse (which we assume to be $\tau_L=10$ ns and having $\Delta\lambda_L=1$ Å), the integration of the relevant rate equation gives us the number of excited argon atoms N^* in the $3p^5 4s'[\frac{1}{2}]^0_1$ level to be

$$N^*=N_0\sigma_{(3)}F^3\tau_L G^{(3)} \quad (12)$$

in cm^{-3}, where $G^{(3)}$ is the three-photon statistical correlation factor 3! Presuming we started with neutral argon atoms $N_0\cong 2.43\times10^{17}$ atoms/cm^3 and assuming an irradiance I of 2×10^8 W/cm^2 we arrive at $N^*=8.802\times10^8$ atoms/cm^3.

VII. SUMMARY

Using the standard perturbation theory expression for the transition probability of a three-photon bound-bound excitation, we have computed the generalized three-photon excitation cross section in neutral atomic argon at a wavelength of 3144.67 Å for linearly polarized light. A truncated summation method has been essentially employed in the evaluation of the sums over the virtual intermediate states. For our chosen set of excitation schemes, the maximum value of the three-photon generalized cross section in atomic argon at 3.144.67 Å, with a laser bandwidth of 1 Å, is $\sigma_{(3)}=1.414\times10^{-80}$ cm^6 s^2.

ACKNOWLEDGMENTS

Work done by S. N. Dixit was carried out under the auspices of the U.S. Department of Energy (DOE) by Lawrence Livermore National Laboratory under Contract No. W-7405-Eng-48. We are deeply indebted and grateful to Dr. Greg Fetzer for suggesting and partially funding the problem under DOE Contract No. DE-AC03-86SF16039. We also acknowledge support from DOE Contract No. DE-RA03-86SF16496. We sincerely thank Xuan Xiao Wang and Lisa Hickman for computational assistance in this project.

[1]A. E. Siegman, *Lasers* (University Science, Mill Valley, CA, 1986).

[2]P. Lambropoulos, *Topics on Multiphoton Processes in Atoms Advances in Atomic and Molecular Physics* (Academic, New York, 1976), p. 87.

[3]J. Morellec, D. Normand, and G. Petite, *Nonresonant Multiphoton Ionization of Atoms Advances in Atomic and Molecular Physics* (Academic, New York, 1982), Vol. 18, p.97.

[4]W. B. Westerveld, Th. F. A. Mulder, and J. V. Eck, J. Quant. Spectrosc. Radiat. Transfer **21**, 553 (1979).

[5]R. A. Lilly, J. Opt. Soc. Am. **66**, 245 (1976).

[6]J. B. Shumaker, Jr. and C. H. Popenhoe, J. Opt. Soc. Am. **57**, 1 (1967), p. 8.

[7]W. L. Wiese, M. W. Smith, and B. M. Miles, *Atomic Transition Probabilities (Na through Ca—A Critical Data Compilation),* Natl. Bur. Stand. Ref. Data Ser., Natl. Bur. Stand. (U.S.) Circ. No. 22 (U.S.GPO, Washington, D.C., 1969), Vol. II.

[8]R. D. Cowan, *The Theory of Atomic Structure and Spectra* (University of California Press, Berkeley, 1981).

[9]I. I. Sobelman, *Atomic Spectra and Radiative Transitions* (Springer-Verlag, New York, 1979).